Cell Reports, Volume *33*

Supplemental Information

Dendritic Cells and Microglia Have Non-redundant Functions in the Inflamed Brain with Protective Effects of Type 1 cDCs

Mattia Gallizioli, Francesc Miró-Mur, Amaia Otxoa-de-Amezaga, Roger Cugota, Angélica Salas-Perdomo, Carles Justicia, Vanessa H. Brait, Francisca Ruiz-Jaén, Maria Arbaizar-Rovirosa, Jordi Pedragosa, Ester Bonfill-Teixidor, Mathias Gelderblom, Tim Magnus, Eva Cano, Carlos del Fresno, David Sancho, and Anna M. Planas

Supplementary Fig S1.

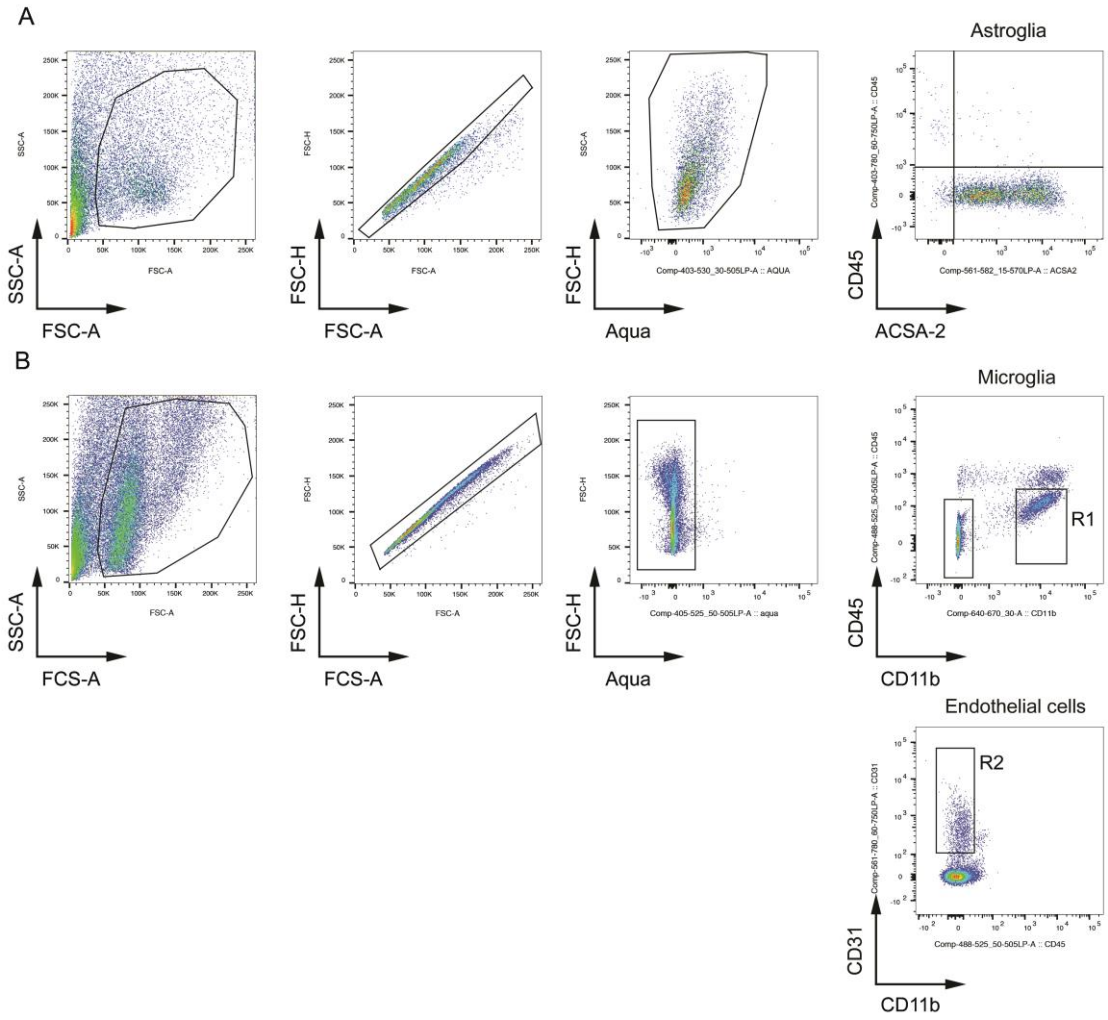

Sup. Fig. S1. Isolation of astroglia, microglia, and endothelial cells from control and ischemic brains. ***Related to Fig. 1F.*** A) Astrocytes were isolated using immunomagnetic separation. We checked the purity by flow cytometry (mean±SD: 92.3±2.7%, n=3) as illustrated in the plots. B) Gating strategy for isolation of microglia and endothelial cells by FACS. Cells were labeled with Aqua Live/Dead staining and CD45, CD11b and CD31 antibodies. After excluding aggregated cells and dead cells, for the microglia gate (R1) we sorted $CD45^{lo}CD11b^{lo}$ cells and for the endothelial cells gate (R2) we sorted $CD45^{-}CD11b^{-}CD31^{+}$ cells. We checked cell purity (n=1 per group): 97.5% for endothelial cells and 92.9% for microglia.

Supplementary Fig. S2

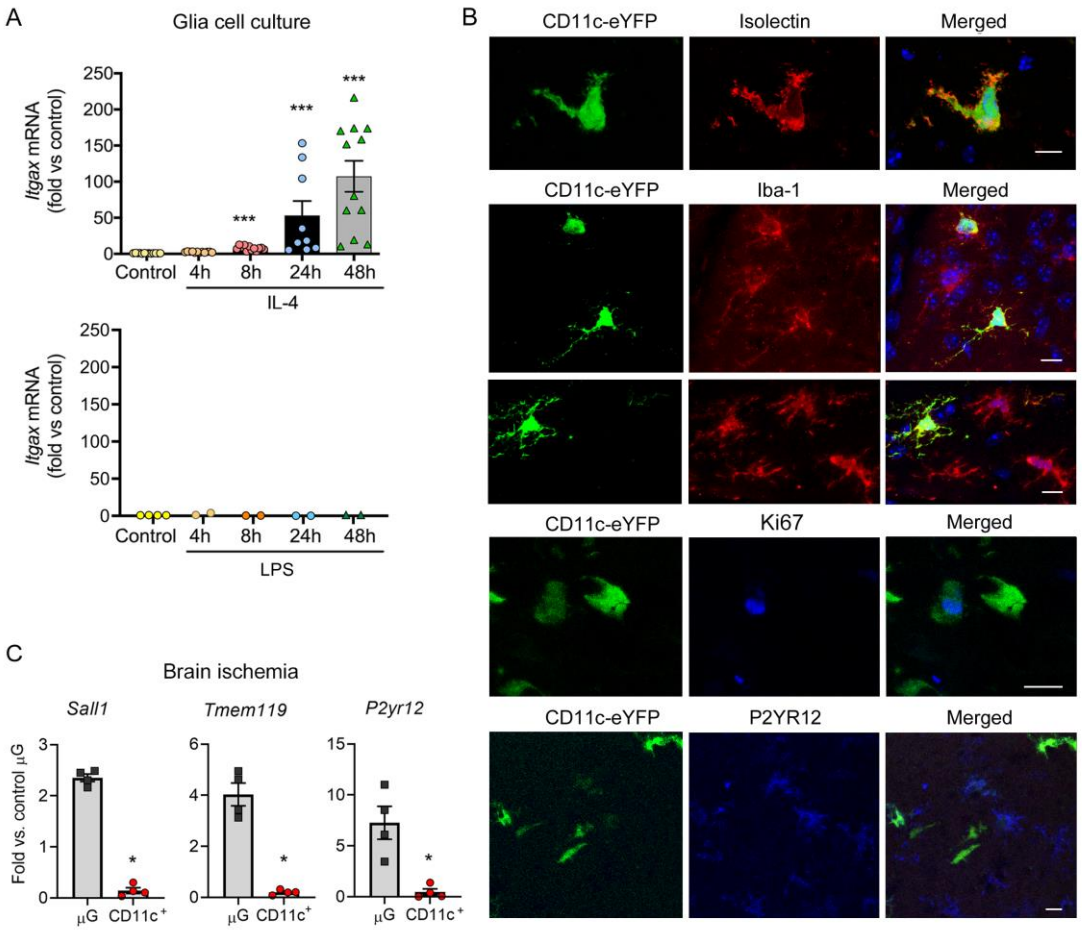

Sup. Fig. 2. **CD11c$^+$ cells in the ischemic brain tissue display features different from microglia** ***Related to Fig. 1C,G***. A) *Itgax* mRNA expression (RT-PCR) in glial cell cultures obtained from postnatal brain of WT mice exposed to mouse recombinant IL-4 (50 ng/mL) or LPS (10 ng/mL). IL-4, but not LPS, induces *Itgax* expression at 8h, 24h and 48h after IL-4 (one-way ANOVA, ***p<0.001, n=9-13 samples per time point, obtained in 4 independent experiments). B) eYFP$^+$ cells (green) 4 days post-ischemia (n=6) are positive for Isolectin and Iba-1 (red); To-Pro3 stained nuclei (blue) are also shown in the corresponding merged images. However, some CD11c-eYFP$^+$ cells are negative for P2YR12 (blue). Scale bar: 10 μm. C) We FACS sorted eYFP$^+$ cells from the brain of CD11c-eYFP mice, and microglia (μG) from the brain of CX3CR1cre^{ERT2}:Rosa26-tdT mice under control conditions and 4 days post-ischemia. We obtained mRNA from the sorted cells and carried out RT-PCR. Values correspond to cells from ischemic mice and are expressed as fold vs. gene expression in microglia from control brain. Expression of typical microglial genes, *Tmem119, Sall1*, and *P2yr12* is lower in CD11c$^+$ cells compared to microglia (Mann-Whitney test, *p=0.029, n=4 mice per group). Bars show the mean±SEM and symbols show the individual values per each mouse.

Supplementary Fig. S3

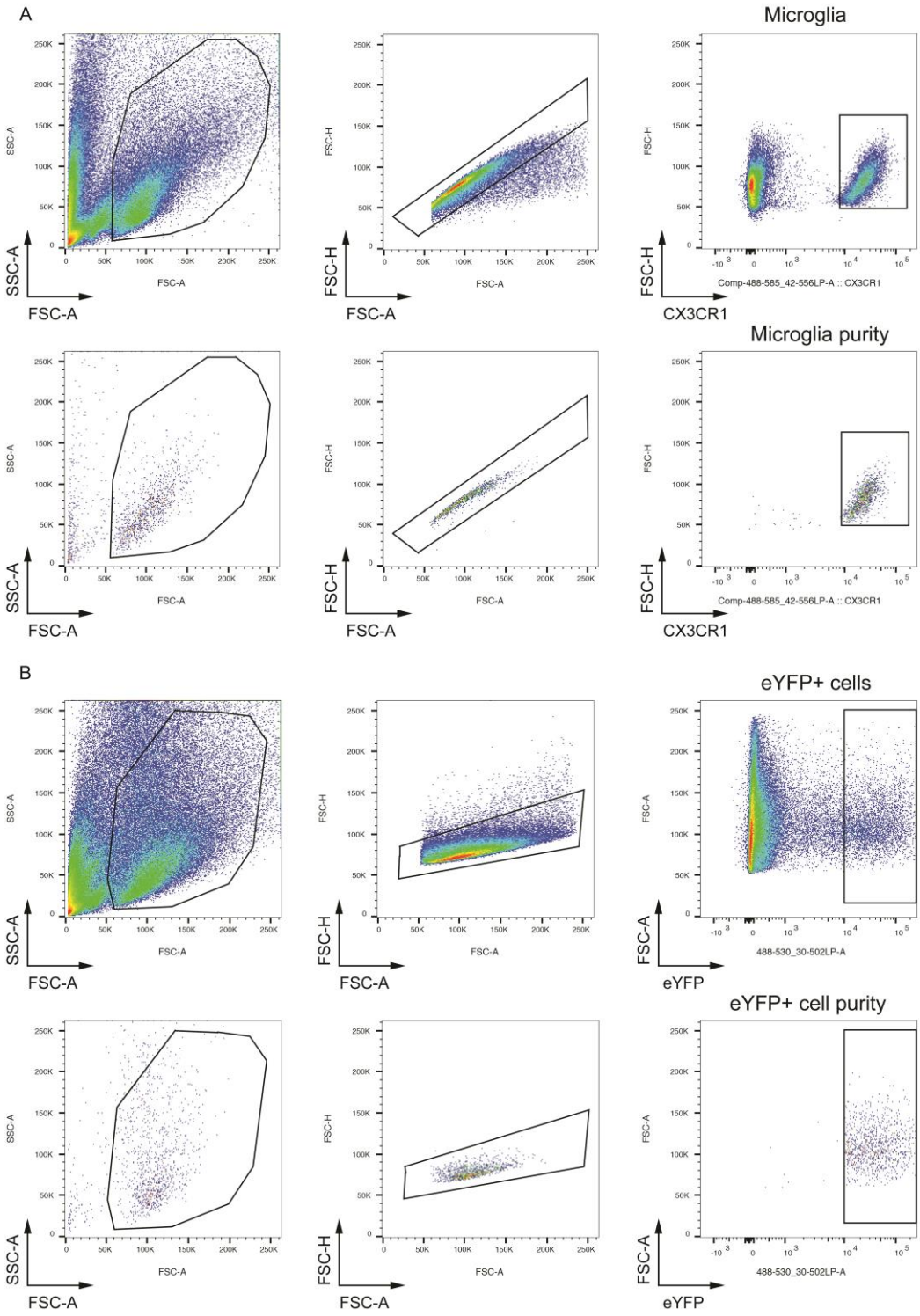

Sup. Fig. S3. Gating strategy for FACS of microglia and CD11c-eYFP^{+} cells. ***Related to Fig. 2A.*** A) Gating strategy for sorting microglia from the brain of CX3CR1cre^{ERT2}:Rosa26-tdT mice. We checked by flow cytometry the purity of sorted microglia: 98.3% (n=1) for control microglia, and 93.9±1.4% (n=2) for ischemic microglia. B) Gating strategy for sorting eYFP^{+} cells from the ischemic brain of CD11c-eYFP mice**.** Purity of eYFP^{+} cells: 86.4%, n=1, as assessed by flow cytometry.

Supplementary Fig. S4

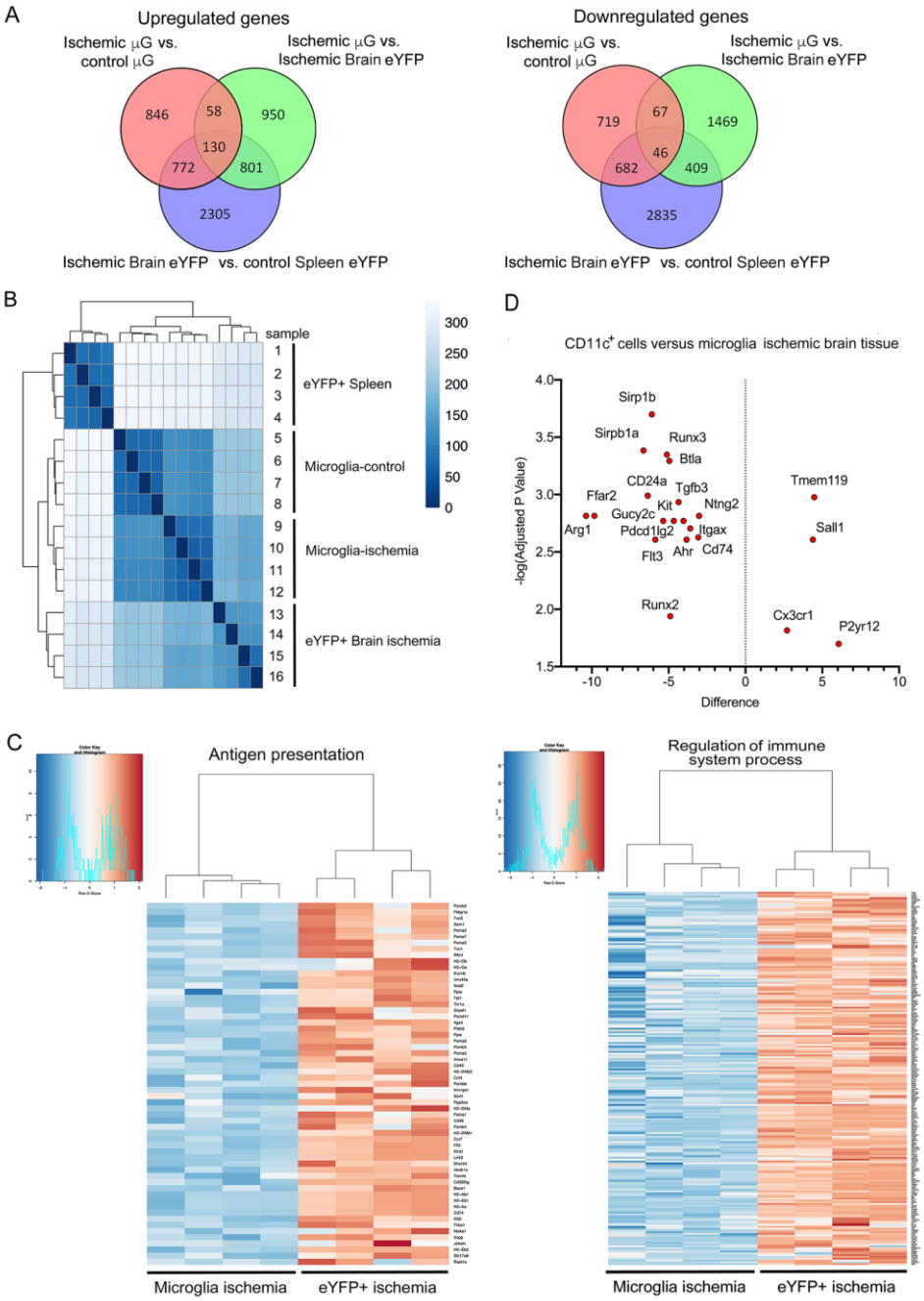

Sup. Fig. S4. Analysis of genes differentially expressed in the various cell populations. ***Related to Fig. 2B, C.*** A) We compared gene expression in microglia (μG) versus eYFP$^+$ cells of the ischemic brain (4 days post-ischemia), and the latter cells with spleen eYFP$^+$ cells. We also compared ischemic versus control microglia. The Venn diagrams show the distribution of upregulated and downregulated genes in each comparison and the overlap between them B) The dendrogram shows separation between the different samples of each cell group (n=4 per group) according to unsupervised analysis. C) Heatmaps of the GO terms: *Antigen presentation* and *Regulation of Immune system process* in the comparison between microglia and eYFP$^+$ cells, both obtained from the ischemic brain tissue. Genes in these terms are significantly overrepresented (red) in eYFP$^+$ cells versus microglia (Log2FC >1.5 adjusted p value <0.001). D) From the RNA-Seq analysis, we selected several genes differentially expressed between CD11c-eYFP$^+$ cells and microglia of the ischemic brain tissue for independent validation by RT-PCR. The selected group of genes clearly separated microglia genes from DC genes, as illustrated in the Volcano plot.

Supplementary Fig. S5

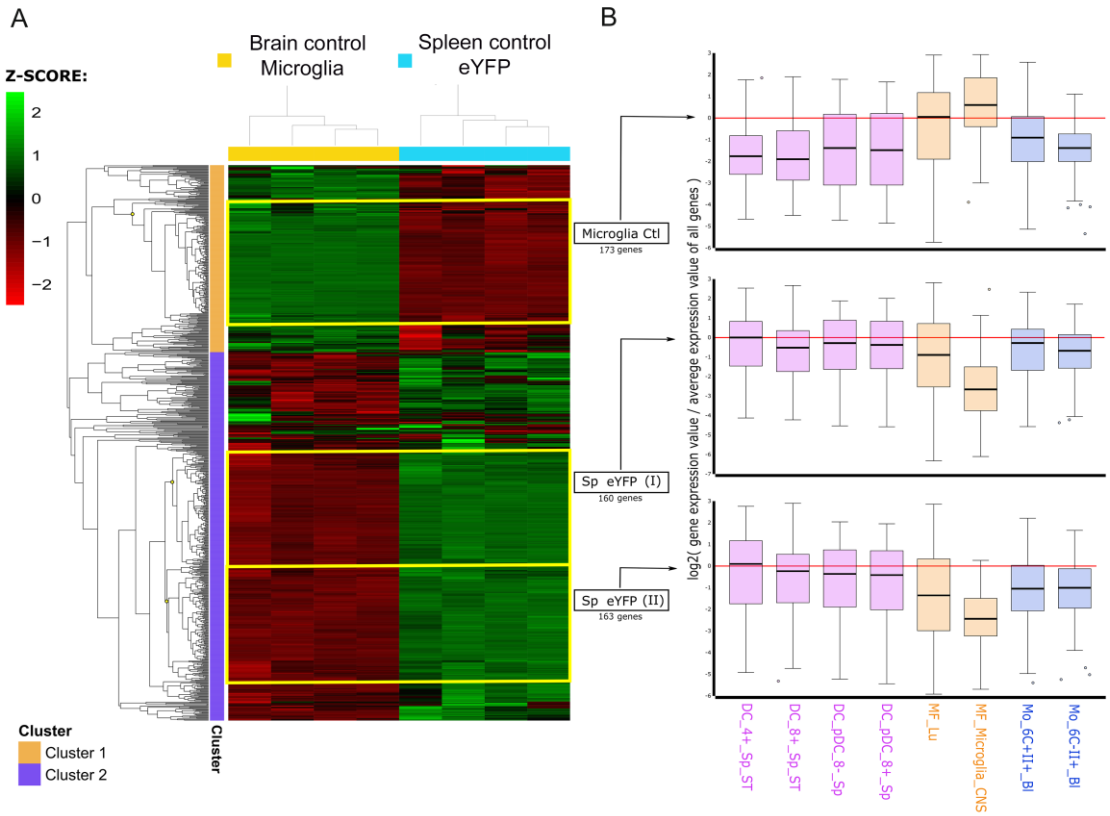

Sup. Fig. S5. Comparison of the transcriptomic data of control brain microglia and control spleen CD11c-eYFP$^+$ cells with ImmGen reference cell population expression profiles. ***Related to Fig. 2C, D.*** A) We compared our RNA-Seq data of Control brain microglia (n=4) and Control spleen eYFP$^+$ cells (n=4) with ImmGen reference cell populations. The comparison retrieved 787 genes that were used to construct a heatmap representation and perform hierarchical clustering. The representation includes two natural clusters found by unsupervised clustering. Clusters correspond to genes upregulated (green) or downregulated (red) in each cell group. Three subclusters were selected due to their differential expression amongst the two studied groups (each marked with a yellow square on the heatmap). Subcluster *Microglia Ctl*. is upregulated in control brain microglia and contains 173 genes. Subclusters *Sp eYFP (I)* and *(II)* are upregulated in control spleen eYFP$^+$ cells and contain 160 and 163 genes, respectively. B) The expression of the genes included in each subcluster was checked on the reference cell populations using the *My Geneset* tool available in ImmGen online resources. The graphs display the generated boxplots for each of the subclusters. The *Microglia Ctl* subcluster is upregulated among the ImmGen macrophage/microglia population (*MF_Microglia_CNS*) and, to a lower extent, among peripheral macrophages (*MF_Lu*). The subclusters corresponding to spleen eYFP$^+$ cells termed *Sp eYFP (I)* and *Sp eYFP (II)* display a slight upregulation in ImmGen splenic CD4$^+$ myeloid DCs (*DC_4+_Sp_ST*) and the remaining DC populations (*DC_8+_Sp_ST, DC_pDC_8-_Sp* and *DC_pDC_8+_Sp*), whereas they were downregulated in ImmGen CNS macrophages/microglia (*MF_Microglia_CNS)*.

Supplementary Fig. S6

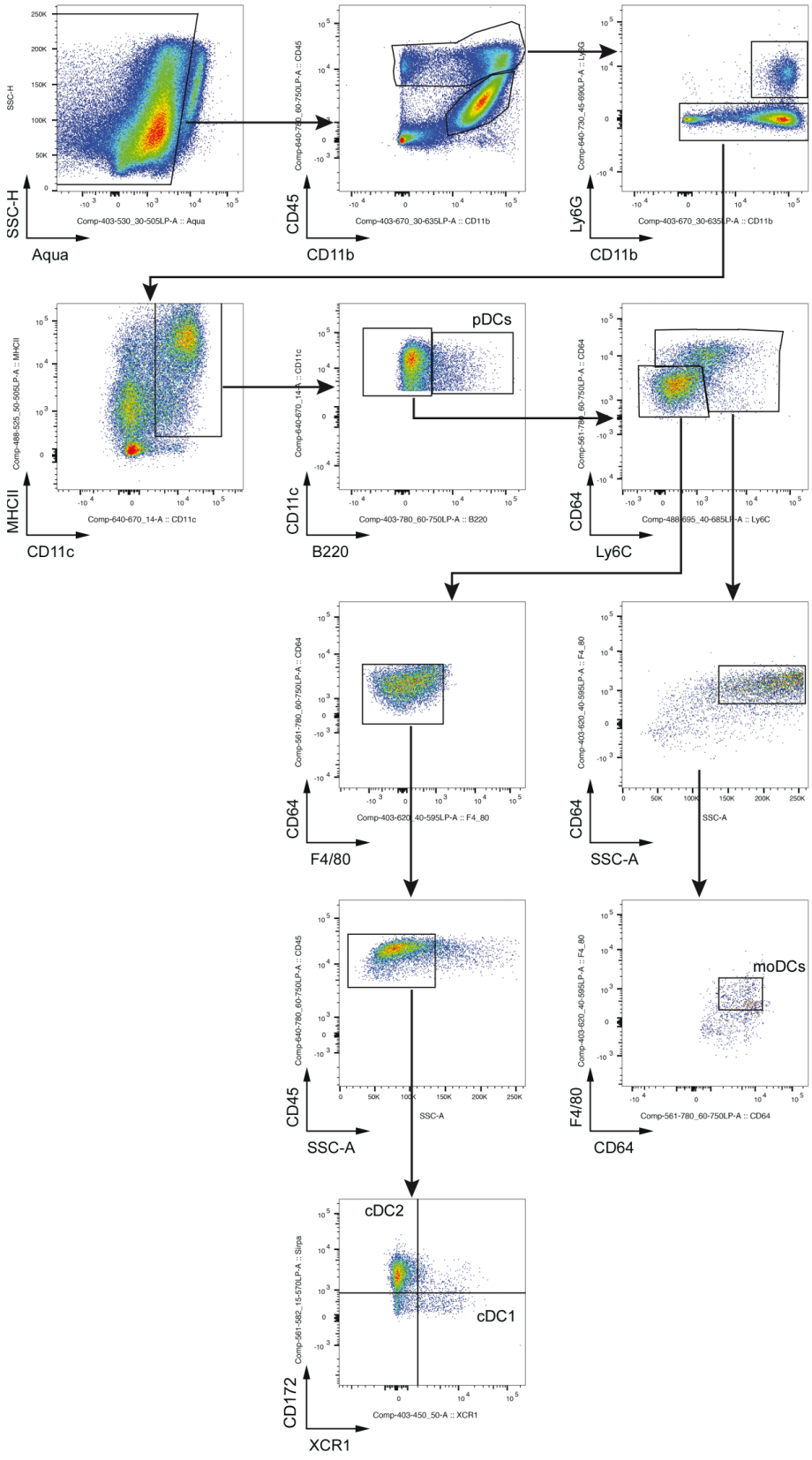

Sup. Fig. S6. Gating strategy. ***Related to Fig. 4F.*** Strategy for DC subsets in WT mouse brain four days post-ischemia.

Supplementary Fig. S7

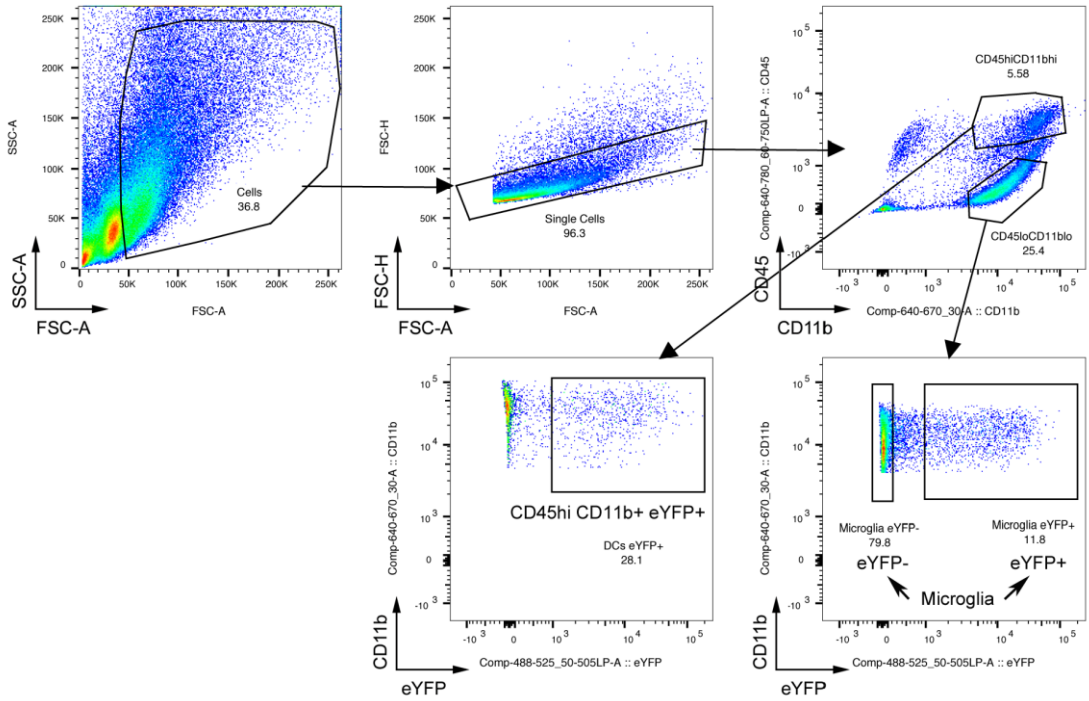

Sup. Fig. S7. Gating strategy. ***Related to Fig. 4H, I.*** Strategy for cell sorting to obtain $CD45^{lo}CD11b^{+}eYFP^{-}$ microglia, $CD45^{lo}CD11b^{+}eYFP^{+}$ microglia, and $CD45^{hi}CD11b^{+}eYFP^{+}$ cells for T cell proliferation assays.

Supplementary Fig. S8

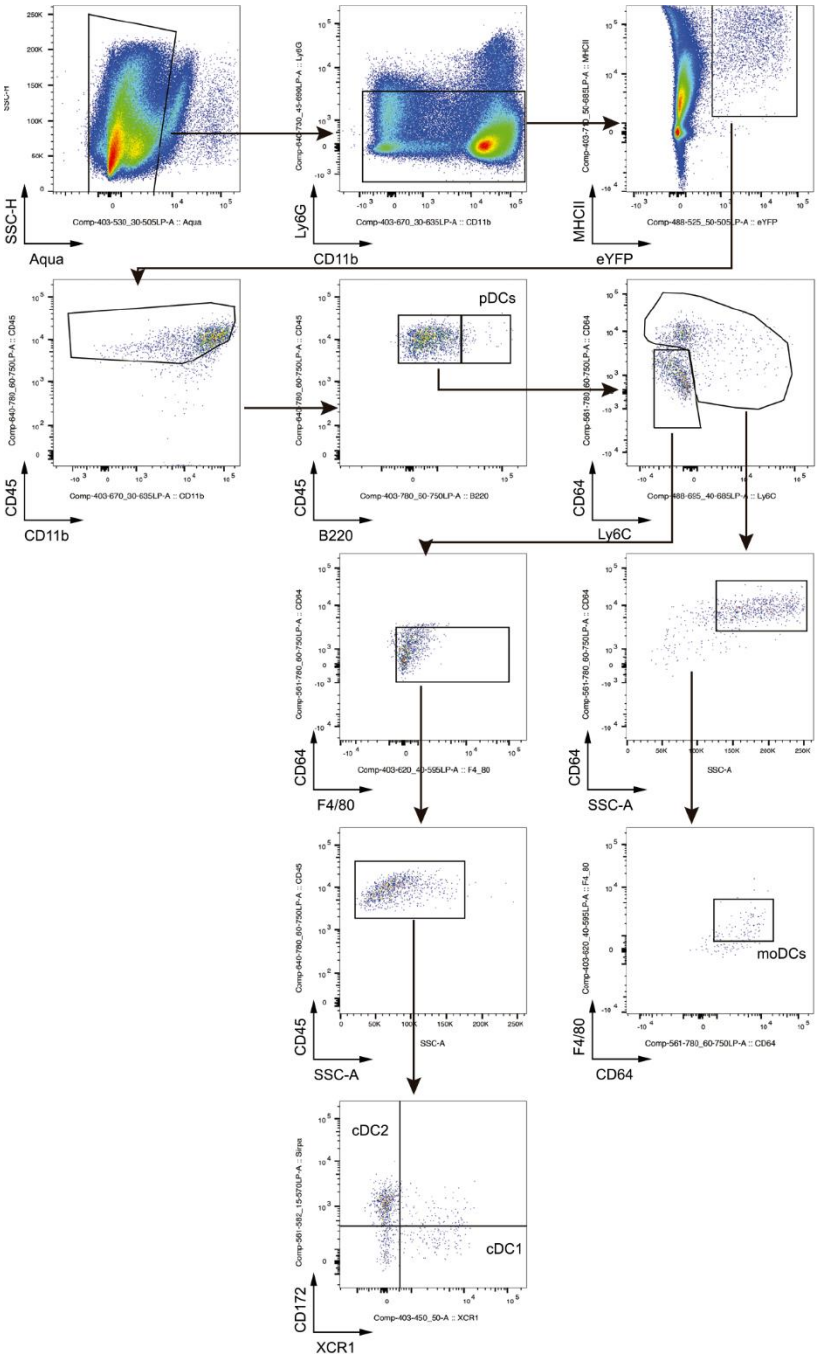

Sup. Fig. S8. Gating strategy for CD11c-eYFP^{+} DC subsets. ***Related to Fig. 5H.*** Data obtained from the brain of ischemic WT parabiotic mice, 4 days post-ischemia. The gating shows cDC1, cDC2, moDCs and pDCs.

Supplementary Fig. S9

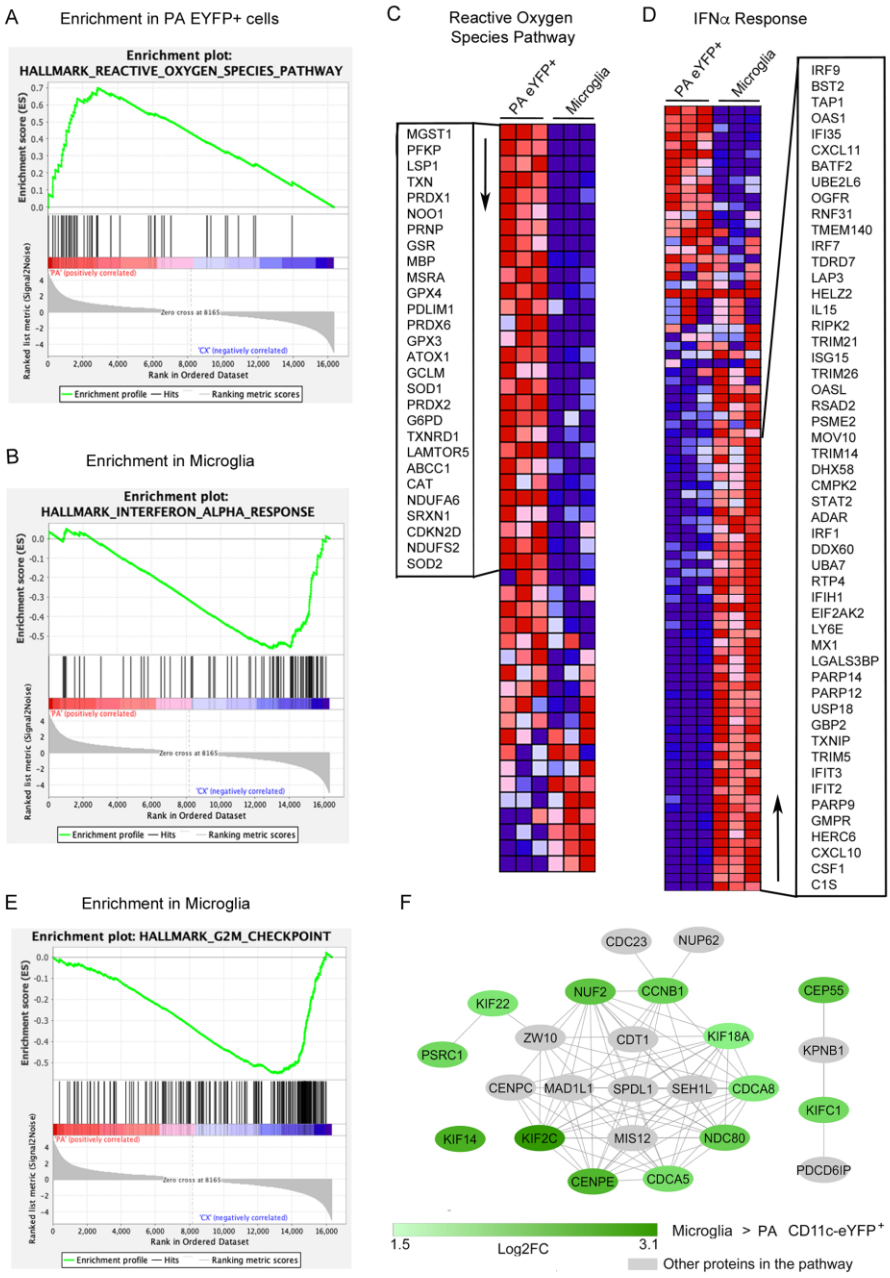

Sup. Fig. S9. Gene Set Enrichment Analysis (GSEA) of the RNAseq of microglia vs. infiltrating eYFP$^+$ cells of parabiotic wild type mice 4 days post-ischemia (PA eYFP$^+$). ***Related to Fig. 5E, G.*** A) Enrichment plot showing the pathway with the highest enrichment score for PA eYFP$^+$ cells, i.e. Reactive Oxygen Species (ROS). B) Respective heat map showing clustered genes in the leading edge subset of the ROS pathway. The range of colors (red, pink, light blue, dark blue) shows the range of expression values (high, moderate, low, lowest). Arrows indicate the direction of the list of genes from high towards low enrichment score. The genes listed in the heat map are those contributing to the leading-edge subset within each gene set. C) Enrichment plot showing the pathway with the highest enrichment score for Microglia, i.e. Interferon-α (IFN-α) response pathway. D) Respective heat map showing the clustered genes in the leading edge subset of the IFN-α response pathway. E) Enrichment plot in microglia showing one of several pathways with genes involved in cell proliferation, that are not enriched in infiltrating PA eYFP$^+$ cells. F) Cytoscape illustration of a protein pathway representative of cell cycle-related processes (GO term: *Mitotic metaphase plate congression)* generated from genes upregulated

in microglia versus infiltrating CD11c-eYFP^{+} cells, and other molecules in the pathway not differentially expressed in our samples (grey).

Supplementary Fig. S10

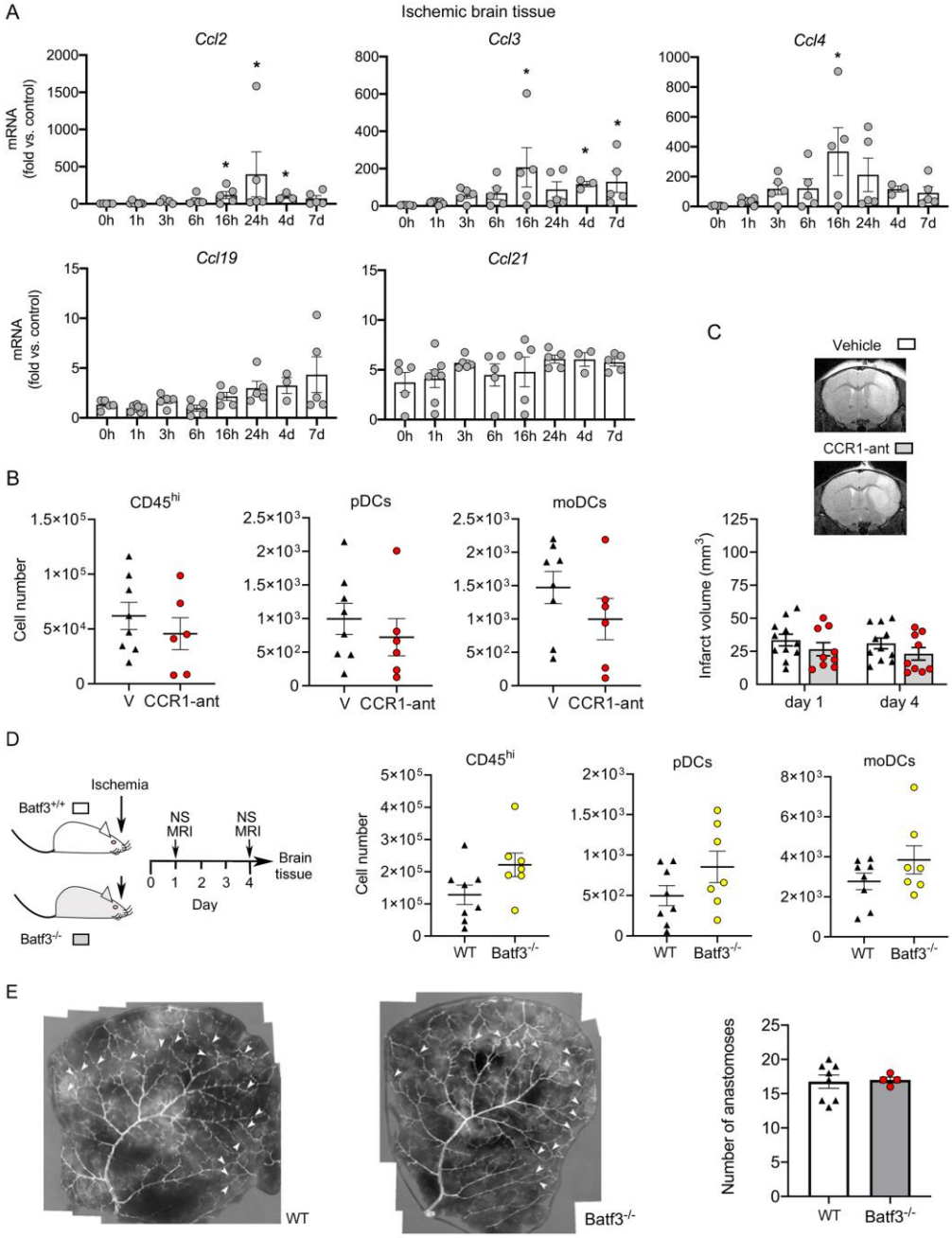

Sup. Fig. S10. In various experimental conditions: DC chemoattraction after ischemia, leukocyte infiltration, and collateral vessels. ***Related to Fig. 6, 7.*** A) Brain chemokine mRNA at several time points post-ischemia (h, hours; d, days), in addition to Ccl5 and Ccl8 mRNA shown in Fig. 6C, (n=3-7 mice per time point), Kruskal-Wallis & Dunn's test (*p<0.05). B) Mice received daily CCR1 antagonist J113863 (CCR1-ant)(10 mg/Kg, i.p.) or vehicle (V) starting 1 day post-ischemia and up to day 3. Brain tissue was studied at day 4 by flow cytometry in mice treated with CCR1-ant (n=6) or V (n=8). Treatment did not affect the number of CD45^{hi} cells, pDC or moDCs in the ischemic tissue. C) Representative MRI (Turbo-RARE) images of the brain lesion 1 day post-ischemia, i.e. before treatment, show similar lesion volume in both groups. Four mice per group died and were excluded. The treatment did not modify the volume of infarction at day 4 post-ischemia (V n=11 mice; CCR1-ant n=10 mice). D) Brain tissue of *Batf3*$^{-/-}$ (n=8) and WT (n=8) mice 4 days post-ischemia showed no group differences in CD45^{hi} cells, pDCs or moDCs. E) *Batf3*$^{-/-}$ mice have a cerebrovascular anatomy similar to that of WT mice. Counting the number of vascular anastomoses (arrowheads) on the brain surface showed comparable values in *Batf3*$^{-/-}$ mice (n=4) and WT mice (n=8). Measures were carried out in a blinded fashion. An independent researcher validated the results with a significant inter-observer correlation (**p<0.007, Pearson r=0.73).

SUPPLEMENTARY TABLES

Sup. Table S1. Functional annotation clustering showing functions overrepresented in CD11c-eYFP^{+} cells vs. microglia. ***Related to Fig. 2C***

	Enrichment Score	Annotation Clusters	Count	%	Fold Enrichment	Benjamini	FDR
1	8,776	Cell-cell adherens junctions	67	3,59	2,428	2,14E-09	2,60E-08
		Cadherin binding in cell-cell adhesion	60	3,21	2,411	1,80E-07	4,31E-07
		Cell-cell adhesion	39	2,09	2,347	1,60E-03	1,97E-03
2	2,834	Phosphorylation	85	4,55	1,579	1,68E-02	4,86E-02
		Kinase activity	90	4,82	1,497	1,38E-02	1,67E-01
		Transferase activity	172	9,21	1,310	1,52E-02	2,19E-01
		Protein autophosphorylation	32	1,71	1,989	7,53E-02	5,44E-01
		Protein phosphorylation	74	3,96	1,461	1,50E-01	1,71E+00
		Protein kinase activity	68	3,64	1,436	1,35E-01	3,59E+00
		Protein serine/threonine kinase activity	54	2,89	1,415	3,08E-01	1,35E+01
		ATP binding	148	7,92	1,101	8,40E-01	8,78E+01
		Nucleotide binding	187	10,01	1,083	8,63E-01	9,20E+01
3	2,615	MHC class II protein complex	10	0,54	9,543	3,74E-06	7,56E-05
		Intestinal immune network for IgA produ.	17	0,91	4,194	1,96E-04	9,39E-04
		Antigen process /presentation peptide MHC II	9	0,48	7,311	5,94E-03	1,22E-02
		Antigen proc. pres. peptide or polysac MHC II	7	0,37	8,845	1,73E-02	5,73E-02
		Rheumatoid arthritis	21	1,12	2,654	3,95E-03	9,48E-02
		MHC class II protein complex binding	8	0,43	5,980	1,56E-02	2,45E-01
		Tuberculosis	33	1,77	1,943	1,34E-02	3,87E-01
		Leishmaniasis	16	0,86	2,591	2,67E-02	1,16E+00
		Toxoplasmosis	23	1,23	2,109	2,70E-02	1,30E+00
		Inflammatory bowel disease	15	0,80	2,635	2,59E-02	1,50E+00
		Asthma	9	0,48	3,886	2,52E-02	1,70E+00
		Antigen processing and presentation	17	0,91	2,148	6,08E-02	5,84E+00
		Antigen processing and presentation	11	0,59	2,317	6,12E-01	2,89E+01
		Staphylococcus aureus infection	11	0,59	2,280	1,73E-01	2,25E+01
		Chaperone mediated protein folding cofactor	5	0,27	4,374	6,64E-01	3,46E+01
		Allograft rejection	10	0,54	1,850	3,66E-01	6,93E+01
		Influenza A	23	1,23	1,394	3,80E-01	7,42E+01
		Graft-versus-host disease	9	0,48	1,793	4,17E-01	8,23E+01
		Viral myocarditis	12	0,64	1,574	4,36E-01	8,54E+01
		Autoimmune thyroid disease	11	0,59	1,605	4,43E-01	8,67E+01
		Type I diabetes mellitus	9	0,48	1,504	5,88E-01	9,75E+01
		Phagosome	20	1,07	1,191	6,53E-01	9,93E+01
		Systemic lupus erythematosus	16	0,86	1,128	7,50E-01	1,00E+02
4	2,448	Proteasome core complex	9	0,48	5,153	6,00E-03	2,44E-01
		Threonine-type endopeptidase activity	9	0,48	4,387	4,47E-02	9,26E-01
		Proteasome	12	0,64	2,763	4,41E-02	3,82E+00
		Antigen proc. pres. exogenous peptide MHC I	9	0,48	3,412	2,87E-01	6,45E+00
		Proteasome core complex, α-subunit complex	5	0,27	6,362	7,39E-02	7,48E+00
		Proteolysis cellular protein catabolic process	12	0,64	2,394	5,10E-01	1,71E+01
		Endopeptidase activity	18	0,96	1,802	4,49E-01	2,90E+01
		Proteasome complex	12	0,64	2,082	2,25E-01	3,38E+01

Sup. Table S2. Enrichment analysis in Parabiotic CD11c-eYFP^{+} cells vs. microglia in the ischemic brain tissue of wild type mice. ***Related to Fig. 5E.***

gene_name	log2FoldChange	padj
Htr7	12,66	4,14E-21
Fam83f	11,34	2,09E-18
Cdh1	10,99	2,43E-31
Cdh17	10,76	4,49E-09
Chil3	10,69	3,13E-19
S100a9	10,58	4,29E-05
Ffar2	10,42	7,37E-15
F7	10,30	3,11E-39
B3gnt5	10,18	7,21E-18
F10	10,14	2,90E-15
Ltf	10,08	1,84E-06
H2-Eb2	9,81	2,69E-08
Ifitm1	9,70	3,61E-50
P2ry10	9,67	8,40E-62
Slc16a14	9,59	2,75E-11
Gm9733	9,58	1,33E-12
Napsa	9,50	1,12E-92
S100a8	9,45	2,28E-07
Il1r2	9,44	2,50E-58
Lad1	9,38	1,56E-06
Epcam	9,33	4,27E-17
Spsb4	9,17	5,28E-12
Sgms2	9,09	2,93E-12
Gcsam	8,88	1,48E-12
Gpr171	8,88	6,49E-63
Pkp3	8,79	1,95E-17
Zdhhc15	8,79	4,06E-11
Dpp4	8,75	5,81E-45
Wnt11	8,75	6,17E-11
Cd24a	8,75	1,26E-62
Anxa1	8,66	8,37E-123
Tnfsf4	8,59	5,44E-18
Klri1	8,58	9,96E-09
Gpr141	8,48	7,10E-44
Gpr33	8,43	7,02E-09
Cd177	8,41	1,82E-17
Kcne3	8,19	1,19E-08
Ocstamp	8,14	3,79E-35
Ramp3	8,07	7,69E-16
Ppbp	8,07	5,90E-06
Acpp	8,04	3,98E-17
Scin	8,02	5,66E-10
Dcstamp	8,02	8,99E-38
Apol7c	7,93	8,99E-07
Ceacam19	7,93	6,47E-08
Itgb7	7,92	2,15E-42
Klrk1	7,91	4,70E-44
Alpk2	7,85	1,72E-07
Plbd1	7,85	2,36E-65
Ly6c2	7,83	5,05E-32

Sup. Table S3. Processes highlighted by enrichment analysis in microglia (MG) and/or parabiotic cD11c-eYFP^{+} cells (PA-eYFP) in the ischemic brain tissue. ***Related to Fig. 5E.***

	MG	PA-eYFP
Cell cycle	✓	
- Cell cycle progression	✓	
- Cell division	✓	
- Chromosome formation	✓	
- DNA repair mechanisms	✓	
Neuronal function	✓	
- Cognitive function	✓	
- Synaptic function	✓	
Immune response		✓
- General immune response		✓
- Innate immunity		✓
- Inflammation	✓	✓
- Adaptive immunity		✓
- Cytokine secretion		✓
- Response to toxic substance		✓
- Haematopoiesis		✓
- Leukocyte differentiation		✓
- Immunity-related diseases	✓	✓
Response to cellular stress		✓
- Oxidative stress		✓
Calcium signalling	✓	✓
Migration	✓	✓
- Motility	✓	✓
- Actin biology	✓	✓
- Immune migration and chemotaxis		✓
- Cell adhesion		✓
- Tissue invasion and metastasis		✓

	MG	PA-eYFP
Glial processes	✓	✓
- Microglia activation		✓
- Astroglia activation	✓	
Barrier integrity	✓	✓
- Cell junction	✓	✓
- Extracellular matrix	✓	✓
Hypoxia response and vascular repair	✓	✓
- Response to hypoxia		✓
- Angiogenesis	✓	✓
- Vascular remodelling	✓	✓
- Coagulation		✓
Cell development and differentiation	✓	✓
- Brain development	✓	
- Glial morphogenesis	✓	✓
- Neuronal morphogenesis	✓	
- Neuronal degeneration	✓	
- General cell development	✓	✓
Other enriched processes	✓	✓
- Cardiovascular diseases	✓	✓
- Other diseases	✓	✓
- Cancer-related pathways	✓	✓
- Signalling pathways	✓	✓
- Membrane system		✓
- Protein localization		✓
- Protein polymerization	✓	
- Thermogenesis	✓	✓

MG includes 961 genes and PA-eYFP includes 793 genes with non-corrected p value<0.001 | LOG2FC | >2
Enriched pathways: exclusive MG = 264, exclusive PA-eYFP=595, common=198

Sup. Table S4. Primers used for RT-PCR. ***Related to Star Methods***

Gene Symbol	Gene Name	Assay ID	Ref sequence	Amplicon length	Probe spans exons	Exon Boundary
Ahr	aryl-hydrocarbon receptor	Mm00478932_m1	NM_013464.4	51	yes	3-5
Arg1	arginase 1	Mm00475988_m1	NM_007482.3	65	yes	1-2
Btla	B and T lymphocyte associated	Mm00616981_m1	NM_001037719.2	71	yes	5-6
Ccl2	chemokine (C-C motif) ligand 2	Mm00441242_m1	NM_011333.3	74	yes	1-2
Ccl3	chemokine (C-C motif) ligand 3	Mm00441258_m1	NM_011337.2	78	yes	1-2
Ccl4	chemokine (C-C motif) ligand 4	Mm00443111_m1	NM_013652.2	70	yes	1-2
Ccl5	chemokine (C-C motif) ligand 5	Mm01302427_m1	NM_013653.3	103	yes	1-2
Ccl7	chemokine (C-C motif) ligand 7	Mm00443113_m1	NM_013654.3	122	yes	1-2
Ccl8	chemokine (C-C motif) ligand 8	Mm01297183_m1	NM_021443.3	61	yes	1-2
Ccl19	chemokine (C-C motif) ligand 19	Mm00839966_g1	NM_011888.2	70	yes	1-2
Ccl21	chemokine (C-C motif) ligand 21	Mm03646971_gH	NM_011124.4	91	yes	3-4
Ccr1	chemokine (C-C motif) receptor 1	Mm01216147_m1	NM_009912.4	149	yes	1-2
Ccr2	chemokine (C-C motif) receptor 2	Mm00438270_m1	NM_009915.2	100	yes	2-3
Ccr7	chemokine (C-C motif) receptor 7	Mm01301785_m1	NM_007719.2	78	yes	2-3
Cd24a	CD24a antigen	Mm01191887_g1	NM_009846.2	58	yes	1-2
Cd74	CD74 antigen	Mm00658576_m1	NM_001042605.1	118	yes	1-2
Cx3cr1	chemokine (C-X3-C motif) receptor 1	Mm00438354_m1	NM_009987.4	92	yes	1-2
Ffar2	free fatty acid receptor 2	Mm01176528_g1	NM_001168509.1	81	yes	2-3
Flt3	FMS-like tyrosine kinase 3	Mm00439016_m1	NM_010229.2	108	yes	22-23
Flt3lg	FMS-like tyrosine kinase 3 ligand	Mm00442801_m1	NM_013520.3	95	yes	6-7
Gucy2c	guanylate cyclase 2c	Mm01267705_m1	NM_001127318.1	65	yes	24-25
Hrpt1	hypoxanthine guanine phosphoribosyl transferase	Mm03024075_m1	NM_013556.2	131	yes	2-3
Itgax	integrin alpha X	Mm00498701_m1	NM_021334.2	94	yes	17-18
Kit	kit oncogene	Mm00445212_m1	NM_001122733.1	71	yes	7-8
Ntng2	netrin G2	Mm01325566_m1	AB052336.1 (GenBank)	65	yes	5-6
Pdcd1lg2	programmed cell death 1 ligand 2	Mm00451734_m1	NM_021396.2	95	yes	4-5
P2ry12	purinergic receptor P2Y, G-protein coupled 12	Mm01289605_m1	NM_027571.3	74	yes	2-3
Runx2	runt related transcription factor 2	Mm00501584_m1	NM_001145920.2	91	yes	6-7
Runx3	runt related transcription factor 3	Mm00490666_m1	NM_019732.2	73	yes	4-5
Sall1	sal-like 1	Mm07297700_m1	NM_021390.3	102	yes	3-4
Sirpb1a	signal-regulatory protein beta 1A	Mm02344810_m1	NM_001002898.1	104	yes	4-5
Sirpb1b	signal-regulatory protein beta 1B	Mm02344809_g1	NM_001173460.1	133	yes	3-4
Tgfb3	transforming growth factor, beta 3	Mm00436960_m1	NM_009368.3	60	yes	3-4
Tmem119	transmembrane protein 119	Mm00525305_m1	NM_146162.2	72	yes	1-2